

Identification of γ rays from ^{172}Au and α decays of ^{172}Au , ^{168}Ir , and ^{164}Re

B. Hadinia,^{1,2,*} B. Cederwall,¹ R. D. Page,³ M. Sandzelius,^{1,4} C. Scholey,⁴ K. Andgren,¹ T. Bäck,¹ E. Ganioglu,⁵ M. B. Gómez Hornillos,⁶ T. Grahn,³ P. T. Greenlees,⁴ E. Ideguchi,⁷ U. Jakobsson,⁴ A. Johnson,¹ P. M. Jones,⁴ R. Julin,⁴ J. Juutinen,⁴ S. Ketelhut,⁴ A. Khaplanov,¹ M. Leino,⁴ M. Niikura,⁷ M. Nyman,⁴ I. Özgür,⁵ E. S. Paul,³ P. Peura,⁴ P. Rähkila,⁴ J. Sarén,⁴ J. Sorri,⁴ J. Uusitalo,⁴ and R. Wyss¹

¹*Department of Physics, Royal Institute of Technology, SE-10044 Stockholm, Sweden*

²*University of the West of Scotland, Paisley PA1 2BE, Scotland, United Kingdom*

³*Oliver Lodge Laboratory, University of Liverpool, Liverpool L69 7ZE, United Kingdom*

⁴*Department of Physics, University of Jyväskylä, FIN-40014 Jyväskylä, Finland*

⁵*Science Faculty, Physics Department, Istanbul University, TR-34116 Istanbul, Turkey*

⁶*STFC Daresbury Laboratory, Daresbury, Warrington WA4 4AD, United Kingdom*

⁷*CNS, University of Tokyo, 351-0198 Wako, Japan*

(Received 30 September 2009; published 10 December 2009)

The very neutron deficient odd-odd nucleus ^{172}Au was studied in reactions of 342 and 348 MeV ^{78}Kr beams with an isotopically enriched ^{96}Ru target. The α decays previously reported for ^{172}Au were confirmed and the decay chain extended down to ^{152}Tm through the discovery of a new α -decaying state in ^{164}Re [$E_\alpha = 5623(10)$ keV; $t_{1/2} = 864_{-110}^{+150}$ ms; $b_\alpha = 3(1)\%$]. Fine structure in these α decays of ^{172}Au and ^{168}Ir were identified. A new α -decaying state was also observed and assigned as the ground state in ^{172}Au [$E_\alpha = 6762(10)$ keV; $t_{1/2} = 22_{-5}^{+6}$ ms]. This decay chain was also correlated down to ^{152}Tm through previously reported α decays. Prompt γ rays from excited states in ^{172}Au have been identified using the recoil-decay tagging technique. The partial level scheme constructed for ^{172}Au indicates that it has an irregular structure. Possible configurations of the α -decaying states in ^{172}Au are discussed in terms of the systematics of nuclei in this region and total Routhian surface calculations.

DOI: [10.1103/PhysRevC.80.064310](https://doi.org/10.1103/PhysRevC.80.064310)

PACS number(s): 23.20.Lv, 23.60.+e, 27.70.+q, 29.30.Kv

I. INTRODUCTION

The ^{172}Au nucleus with 79 protons is located at the proton drip line below the $Z = 82$ shell closure. For many nuclei in this region, the emission of α particles from the ground states and low-lying isomeric states enables studies of excited states via the recoil- α tagging technique [1–4]. In addition, detailed nuclear structure information can also be extracted by studies of decays from ground and isomeric states. Several light gold isotopes are also unbound to emission of protons [2,5]. For ^{170}Au and ^{171}Au , the ground states decay predominately by proton emission, whereas the isomeric states have comparable proton and α -decay branches. However, in the heavier Au isotopes, lower proton-decay Q values mean that α -particle emission dominates.

At present, limited knowledge is available on the shape evolution and structure of nuclei in this region. Neither the polarizing effects of the individual proton and neutron orbitals on the nuclear shapes, nor the interactions between valence particles, which are important for the low-lying structures, have been studied sufficiently in this mass region. Experimental studies of odd-odd nuclei can especially provide information on residual interactions and coupling between quasiparticles.

The lightest observed gold isotope is ^{170}Au , for which the level structure is not established. In ^{171}Au only two excited states have been observed using the recoil-proton-

tagging technique [6]. Collective behavior has been found in many odd-even gold isotopes with mass number larger than 173; however, the lightest known odd-odd isotope for which collective behavior has been observed is ^{182}Au [7]. This article reports the first observation of γ rays from excited states in the extremely neutron-deficient odd-odd nucleus $^{172}\text{Au}_{93}$ as well as new α decays from ^{172}Au , ^{168}Ir , and ^{164}Re . Prior to the present work, one α -decaying state in ^{172}Au was reported, but no proton emission was observed for this nucleus [1,8].

II. EXPERIMENTAL DETAILS

The experiments were performed at the Department of Physics JYFL accelerator facility at the University of Jyväskylä, Finland, in three separate runs totaling 320 hours of irradiation time. The ^{78}Kr ions were accelerated by the JYFL $K = 130$ MeV cyclotron to energies of 342 and 348 MeV and used to bombard the 96% enriched self-supporting ^{96}Ru target foils with a thickness of 0.50 mg/cm^2 . A carbon charge reset foil ($50\text{ }\mu\text{g/cm}^2$) was placed immediately downstream of the target. The average beam intensity was 10 pA. Prompt γ rays produced in the reactions were detected by the JUROGAM γ -ray array consisting of 43 EUROGAM [9] type escape-suppressed high-purity germanium (HPGe) detectors distributed over six angles relative to the beam axis. The JUROGAM detector array has a total photopeak efficiency of 4.2% at 1.3 MeV.

The fusion-evaporation products from the $^{96}\text{Ru} + ^{78}\text{Kr} \rightarrow ^{174}\text{Hg}^*$ reaction were separated in flight from the beam particles using the gas-filled recoil separator RITU [10,11].

*baharak.hadinia@uws.ac.uk

The fusion-evaporation residues were implanted into the two double-sided silicon strip detectors (DSSDs) of the GREAT spectrometer [12] at the RITU focal plane. The DSSDs had an active area of $60 \times 40 \text{ mm}^2$ and a strip pitch of 1 mm in both directions, which in total gave 4800 independent pixels. The GREAT spectrometer also includes a multiwire proportional counter (MWPC), an array of 28 silicon PIN diode detectors, a segmented planar germanium detector, and a HPGe clover detector. The recoil discrimination at the focal plane was performed by measuring the energy loss in the MWPC and the time of flight between the MWPC and the DSSDs.

The signals from all detectors were recorded independently, each with a time stamp of 10-ns precision, using the total data readout [13] acquisition system. Spatial and temporal correlations of recoil implants and their subsequent α decays were performed on- and off-line using the GRAIN [14] software package. The highly selective recoil-decay-tagging (RDT) method was applied to select the prompt γ rays corresponding to each implanted recoil. Application of the RDT technique requires the half-lives of the nuclei of interest to be short enough to allow clean correlations even at high implantation rates, but long enough to survive the $\approx 0.5\text{-}\mu\text{s}$ flight time through RITU. The nucleus ^{172}Au , which α decays with a half-life in the millisecond range, is suitable to be investigated using this method.

III. EXPERIMENTAL RESULTS

A. Decays of ^{172}Au and its daughters

Previous studies of α -particle and proton emission in this region have established extensive decay chains involving two distinct states in the gold isotopes ^{170}Au , ^{171}Au , and ^{173}Au [2,5]. In each case, the low-spin ground state is based on a $\pi s_{1/2}$ or $\pi d_{3/2}$ configuration with a higher spin isomeric state based on a $\pi h_{11/2}$ configuration at an excitation energy of 200–300 keV. One would expect a similar pattern for ^{172}Au , with a sequence of consecutive α decays $^{172}\text{Au} \rightarrow ^{168}\text{Ir} \rightarrow ^{164}\text{Re} \rightarrow ^{160}\text{Ta} \rightarrow ^{156}\text{Lu} \rightarrow ^{152}\text{Tm}$. However, prior to this work only a fragmented picture could be established. In ^{156}Lu and ^{160}Ta the higher energy decay lines were found to be correlated [1] and since they were produced more strongly in fusion-evaporation reactions, they were assigned as the $\pi h_{11/2}$ states [1,15]. The lower energy decays from these nuclei were also mutually correlated and further correlated with the only known decay line of ^{164}Re [1]. These decays were therefore assigned as emanating from the low-spin states in these nuclei. The previously reported α decay of ^{172}Au [8] was known to be correlated with the 6.3-MeV decay of ^{168}Ir , but no subsequent correlated decays were observed [1], whereas the 6.2-MeV decay assigned to ^{168}Ir [16] was reported to be correlated with the 5.8-MeV decay line from ^{164}Re [17].

Figure 1 shows the energy spectrum of α particles observed within 18 ms of the implantation of a fusion-evaporation residue into the same DSSD pixel. The previously reported α -decay peak of ^{172}Au is clearly visible. In the present data the correlations through four generations of each decay chain were analyzed. Figures 2(a)–2(d) show the correlation of a

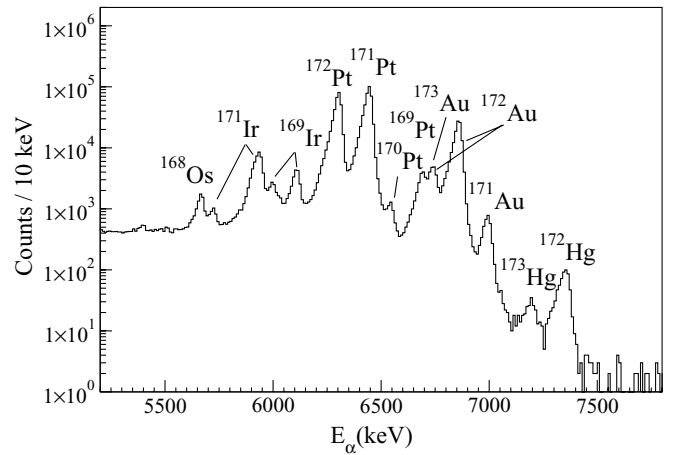


FIG. 1. A total correlated α -particle energy spectrum obtained with a correlation time of up to 18 ms between an implanted recoil and its subsequent α decay in a single pixel of the DSSDs.

new 6762-keV α decay of ^{172}Au with the 6230-keV α decay of its daughter, ^{168}Ir , the 5780-keV α decay of ^{164}Re , and the 5320-keV α decay of the low-spin state in ^{160}Ta . These correlations, taken together with the lower production rate of this ^{172}Au α -decay line in this work and of the 6230-keV ^{168}Ir decay line in Ref. [1], suggest that these decays form the chain connecting the low-spin states. Figures 2(e)–2(h) show the corresponding chain of α decays down to the 5412-keV α decay of the low-lying high-spin state in ^{160}Ta . These spectra reveal first evidence of fine structure in the α decays of ^{172}Au and ^{168}Ir , as well as a new α -decay line at 5623 keV from ^{164}Re . On the basis of systematics, all these α -decaying states in this chain are expected to lie above the ground states of their respective nuclei. The decay schemes for both of these decay chains are summarized in Fig. 3.

The results of the correlation analysis are also displayed as two-dimensional plots in Fig. 4. The mother-daughter correlation matrix [Fig. 4(a)] has been obtained by applying time and energy conditions on the granddaughter decay that is chosen to be the α decay from the isomeric or the ground state in ^{164}Re . Similarly, the daughter-granddaughter matrix [Fig. 4(b)] has been obtained by applying time and energy conditions on the mother decay that is chosen to be the α decay from the isomeric or the ground states in ^{172}Au .

The half-lives of the studied α -decaying states have been derived using the maximum likelihood method. In Table I the energies and half-lives of the α decays studied in the present work are listed and compared with available literature values. The α -decay branching ratios b_α are also presented for the high-spin decay chain. It was not possible to extract reliable values for the low-spin chain owing to interference from the decay chain of ^{169}Pt , as can be seen from Fig. 2(d).

Further investigations into the fine structure of the α decay of the isomeric state in ^{168}Ir and ^{172}Au have been carried out by studying the events for which recoil-correlated α decay in the DSSDs were followed by γ rays detected by the germanium detectors of GREAT located at the focal plane of RITU. Figure 5 displays the focal plane γ -ray energy spectrum gated by the α decay with energy 6260 keV ($^{168}\text{Ir}^{(m)}$) applying a

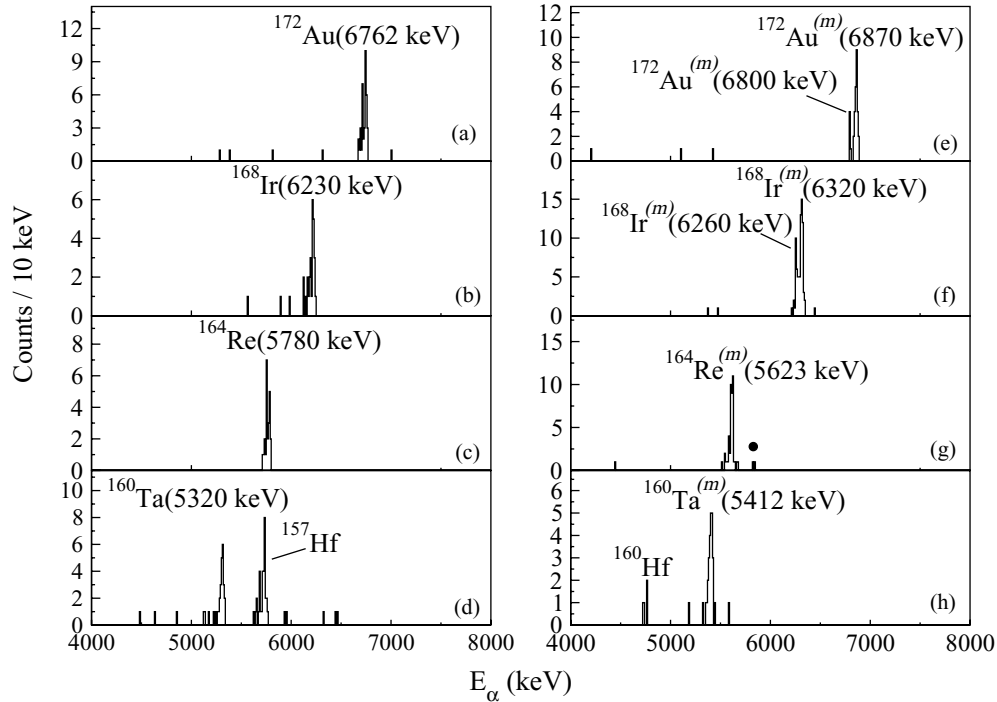


FIG. 2. Alpha-particle energy spectra originating from the ground states (left plots) and isomeric states (right plots) in the α -decay chains that begin with ^{172}Au and end with ^{156}Lu . The spectra have been extracted from the recoil-mother-daughter-granddaughter-great granddaughter correlations in each decay chain. Each α spectrum is obtained by applying energy conditions on α particles from the three other members of the decay chain as well as setting time conditions ($\sim 3t_{1/2}$) on the decays of all four members. The α peak belonging to the decay of ^{157}Hf appears in the spectrum (d) due to partial overlapping of the α -particle energies in its decay chain with the decay chain of interest (^{172}Au - ^{168}Ir - ^{164}Re - ^{160}Ta). The nucleus ^{160}Hf , the decays of which are seen in (h), is populated via β decay of ^{160}Ta . The solid circle (g) is placed to point out the possibility that a weak 5846-keV line might be assigned to the highest energy α decay emanating from $^{164}\text{Re}^{(m)}$ (see the discussion section for more details).

correlation time between recoil implantation and α -particle detection of about three times the half-life of the α -decaying state in ^{168}Ir . A γ -ray peak at an energy of 69.0(4) keV is visible (see Fig. 5), which is consistent with the 61 ± 10 -keV difference between the Q values of α decays emanating from the isomeric state in ^{168}Ir . The electron binding energy in the

K shell in rhenium is about 72 keV implying that the 69.0(4) transition cannot be converted via K shell.

A similar analysis of the fine structure in the α decay of ^{172}Au shows the correlation of 6800-keV α particles with a 65.0(4)-keV line in the γ -ray spectrum (see Fig. 6), which is also consistent with the 71 ± 10 -keV difference in Q values of

TABLE I. Summary of α -decay measurements from the present work in comparison with literature values, where available. The asterisks indicate new observed decay data deduced from the present work.

Nuclide	E_α (keV)		$t_{1/2}$ (ms)		b_α (%)	
	Present work	Literature	Present work	Literature	Present work	Literature
$^{172}\text{Au}^{(m)}$	6870 ± 10	6878 ± 9 [1] 6860 ± 10 [8]	9_{-1}^{+2}	6.3 ± 1.5 [1] 4 ± 1 [8]		
$^{172}\text{Au}^{(m)*}$	$6800 \pm 10^*$		8_{-2}^{+5} *			
$^{172}\text{Au}^*$	$6762 \pm 10^*$		22_{-4}^{+6} *			
$^{168}\text{Ir}^{(m)}$	6320 ± 10	6323 ± 8 [1]	160_{-20}^{+30}	161 ± 21 [1]	$53 \pm 5\%^*$	$82 \pm 14\%$ [1]
$^{168}\text{Ir}^{(m)*}$	$6260 \pm 10^*$		153_{-30}^{+40} *		$22 \pm 10\%^*$	
^{168}Ir	6230 ± 10	6227 ± 15 [16]	222_{-40}^{+60}	125 ± 40 [1]		
$^{164}\text{Re}^{(m)*}$	$5623 \pm 10^*$		864_{-110}^{+150} *		$3 \pm 1\%^*$	
^{164}Re	5780 ± 10	5784 ± 7 [1] 5778 ± 10 [18]	848_{-105}^{+140}	380 ± 160 [1] 900 ± 700 [18]		

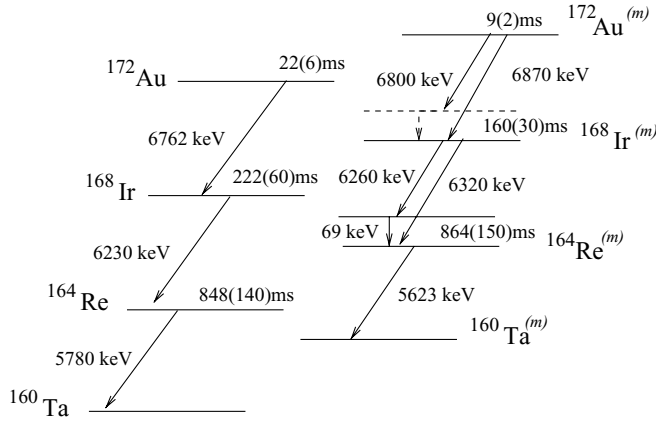


FIG. 3. The decay schemes for the isomeric and the ground-state decay chains that begin with ^{172}Au are shown as far as ^{160}Ta . The label *m* indicates the isomeric chain. For more details see the text and Table I.

the corresponding α -decay states in ^{172}Au (Fig. 6). However, the K_α x-ray energy for iridium is about 65 keV with a total 74% of K-shell vacancies and the K_β x-ray is 73 keV with 20% of K-shell vacancies. In addition to the 65.0(4)-keV line, a weak line at 73.0(6) keV is also seen in the γ -ray spectrum in coincidence with the 6800-keV α branch (with a relative intensity ratio of about 3:1). Therefore, it is most likely that the lines at 65.0(4) and 73.0(6) keV are in fact x rays produced via electron conversion of a highly converted γ ray at a somewhat higher energy (within the limits allowed by the uncertainty of the Q -value difference). Considering that the K-shell electron binding energy for K-shell iridium is about 76 keV, the observation of K x rays in Fig. 6 sets a lower

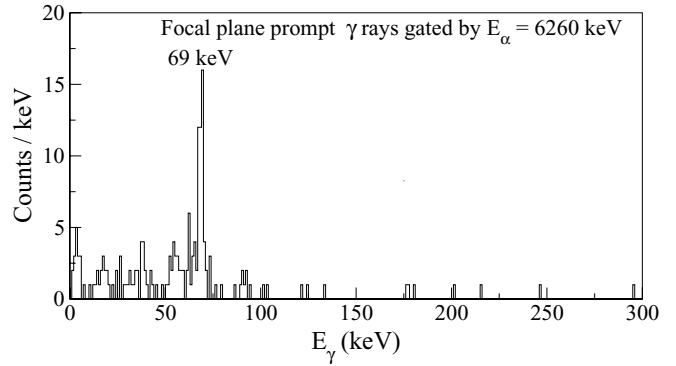


FIG. 5. Gamma-ray energy spectrum obtained from the germanium detectors at the focal plane of RITU following the detection of 6260-keV α particles in the DSSDs, with the implantation of recoils using a 470-ms correlation time.

limit on the energy of the proposed highly converted γ -ray transition.

For an 80-keV γ ray, the K-shell conversion coefficients for transitions of $E1$, $E2$, and $M1$ multipolarity are 0.56, 0.79, and 9.5, respectively. Thus, assuming a γ -ray energy of about 80 keV with $M1/E2$ character its absence in the Fig. 6 spectrum could be explained by a large conversion coefficient. These observations can be used as further proof of the existence of fine structure in the α decays of ^{168}Ir and ^{172}Au as well as proposing the excited state at 69 keV above the metastable state in ^{164}Re and larger than 76 keV (with the upper limit allowed by the uncertainty of the Q -value difference) above metastable state in ^{168}Ir .

The light gold isotopes have previously been proposed to be unbound to proton emission [19] and for ^{170}Au and ^{171}Au the emission of protons has been observed [2,5,20]. A search

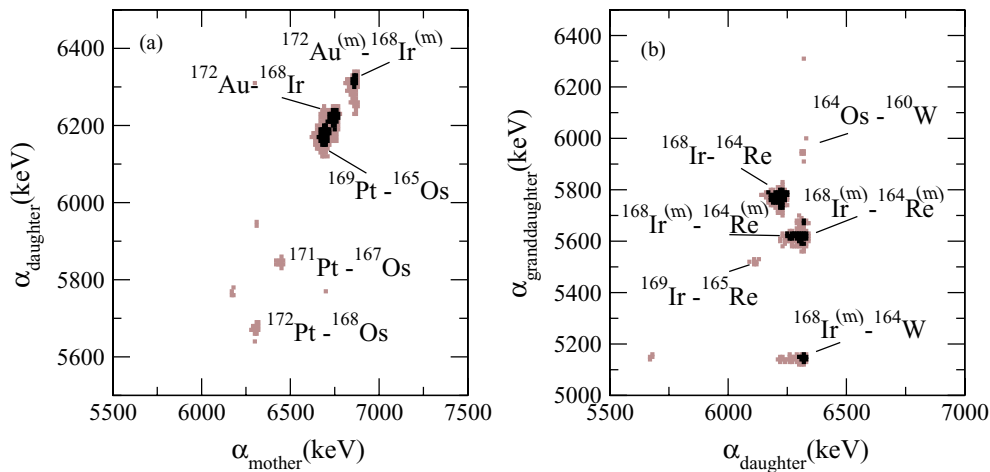


FIG. 4. (Color online) Two-dimensional plots of correlated α decays. (a) The mother-daughter α -particle energies whose granddaughter α decay originates from the isomeric state or the ground state in ^{164}Re . The ^{169}Pt - ^{165}Os pair appears since their granddaughter decay has similar energy to the ground-state decay of ^{164}Re . The presence of the pairs ^{171}Pt - ^{167}Os and ^{172}Pt - ^{168}Os are due to random correlations because of the intense population of ^{171}Pt and ^{172}Pt in this experiment. The brown squares represent more than 10 counts in a point and the black squares represent more than 40 counts. (b) The daughter-granddaughter α -particle energies when the mother decay originates from the isomeric or the ground state in ^{172}Au . The $^{168}\text{Ir}^{(m)}$ - ^{164}W correlation appears due to the β -decay branch of ^{164}Re . The ^{169}Ir - ^{165}Re and ^{164}Os - ^{160}W pairs appear since their mother decay has similar energy to the isomeric state decay of ^{172}Au . The points shown with brown and black squares correspond to more than 5 and 15 counts, respectively.

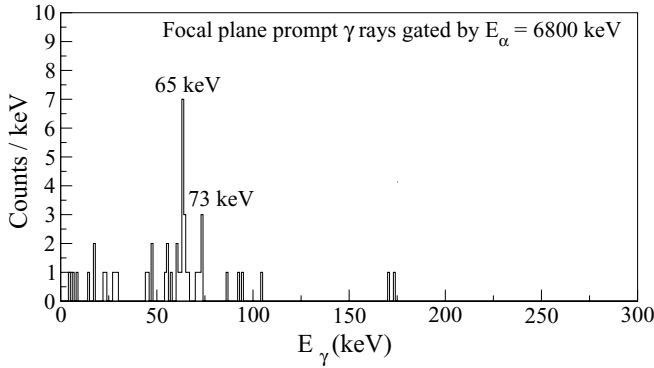


FIG. 6. Gamma-ray energy spectrum obtained from the germanium detectors at the focal plane of RITU following detection of 6800-keV α particles in the DSSD, which are correlated with implantation of recoils using a 20-ms correlation time.

for a proton decay branch in ^{172}Au has been made by Sellin *et al.* [8]. No evidence was found for such a decay mode and an upper limit for the proton decay branching was set at 2%. The partial half-life of proton decay was consequently suggested to be significantly longer than that for α emission ($t_{1/2,p} \geq 200$ ms). In the present experiment a new search for proton decays associated with ^{172}Au recoils has been carried out by examining the correlation between the α decay of ^{171}Pt (6453 keV) and any preceding decay. However, no evidence for proton emission from ^{172}Au has been found in the present experiment and an upper limit for the proton decay branching ratio from the isomeric decaying state in ^{172}Au is estimated to be 0.02%, which is two orders of magnitude smaller than the limit previously estimated by Sellin *et al.* [8].

B. In-beam γ -ray spectroscopy of ^{172}Au

The prompt γ -ray energy spectrum correlated with the 6870-keV α decay of $^{172}\text{Au}^{(m)}$ is shown in Fig. 7. The γ -ray transitions assigned to depopulate the level structure built on the isomeric state in ^{172}Au , their intensities, and their angular distribution ratios (where possible to measure) are listed in Table II.

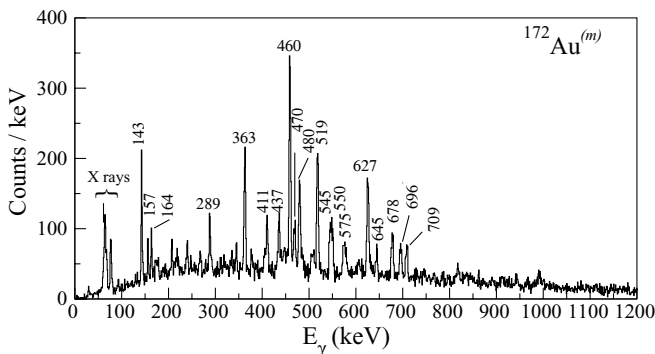


FIG. 7. Recoil- α correlated prompt γ -ray spectrum tagged with the 6870-keV α decay of $^{172}\text{Au}^{(m)}$ applying a correlation time of up to 20 ms between recoil implantation and α -particle detection in the DSSD.

TABLE II. The γ rays assigned to $^{172}\text{Au}^{(m)}$ (upper part of the table) and ^{172}Au (lower part of the table). Statistical uncertainties are given within parentheses. The γ -ray intensities are adjusted for detection efficiency and normalized to the intensity of the strongest γ -ray transition (460 keV for transitions above the isomeric state and 353 keV for transitions above the ground state). Doublet transitions are labeled with asterisks. Angular distribution ratios obtained from $I(157^\circ)/I(94^\circ + 86^\circ)$ and the corresponding types of the transitions are suggested.

Energy (keV)	Relative intensity (%)	Angular distribution ratios	Transition type
143.2(8)	26(2)		
156.6(2)	9(1)		
164.1(2)*	9(1)		
207.8(2)	6(1)		
240.4(2)	7(1)		
268.1(3)	≤ 5		
288.7(1)	14(2)	0.62(12)	$M1$ or $E1$
335.4(5)	≤ 5		
345.4(3)	7(2)		
363.4(7)*	47(2)	1.02(8)	$M1/E2$
377.9(4)	≤ 5		
406.2(4)	7(2)		
411.0(2)	22(2)	0.63(15)	$M1$ or $E1$
436.5(2)	26(2)		
459.7(6)*	100(4)	1.09(6)	$M1/E2$
469.5(2)	25(9)		
480.4(1)	45(2)		
509.0(4)	10(2)		
518.6(1)	63(3)	0.69(7)	$M1$ or $E1$
545.4(3)	21(2)		
549.9(2)	22(2)		
575.0(3)	18(2)		
578.9(8)	≤ 6		
606.6(7)	≤ 5		
626.9(1)	61(3)	1.30(12)	$E2$
644.8(4)	13(2)		
678.2(3)	28(2)		
696.0(3)	21(2)		
708.9(3)	21(3)	0.72(22)	$M1$ or $E1$
818.3(6)	7(2)		
913.1(10)	7(2)		
943.6(10)	7(2)		
991.6(5)	11(2)		
115.6(3)	36(18)		
214.7(3)	80(35)		
351.9(3)	100(34)		

Since the new α decay from ^{172}Au with an energy of 6762 keV observed in this work overlaps with the known α -decay energy of $^{173}\text{Au}^m$, an identification of the excited states built on the ground state in ^{172}Au cannot be made solely by gating on its corresponding α -decay energy. Figure 8(a) displays the γ -ray energy spectrum tagged by recoils that are correlated with the α decay of $^{173}\text{Au}^m$. This spectrum contains the prompt γ rays feeding the ground state of ^{172}Au . Although several γ rays were previously assigned to $^{173}\text{Au}^m$ by Kondev *et al.* [21], its γ -ray energy spectrum was also extracted in

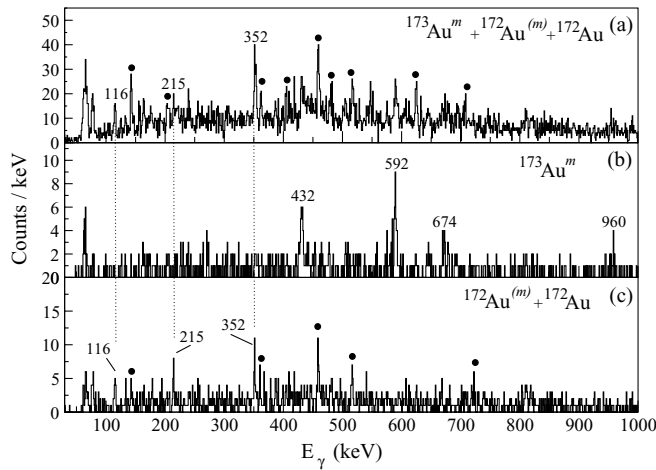


FIG. 8. (a) The γ -ray energy spectrum tagged by recoils correlated with the α -decay energy of $^{173}\text{Au}^m$. (b) The recoil-mother-daughter correlated tagged γ -ray spectrum for $^{173}\text{Au}^m$ is displayed. (c) The recoil-decay mother-daughter correlated tagged γ -ray spectrum for the ground state of ^{172}Au . The γ -ray transitions assigned to ^{172}Au are labeled with their corresponding energy values (keV) in (a) and (c). The solid circles indicate the most intense γ rays from $^{172}\text{Au}^m$.

the present work for comparison, applying mother-daughter correlations, and is shown in Fig. 8(b). Having knowledge of the γ rays of $^{173}\text{Au}^m$ and $^{172}\text{Au}^m$ (which also appear in this gate due to partial overlap of α energies) it is possible to identify the γ rays belonging to the structure built on the ground state in ^{172}Au . Figure 8(c) also displays the mother-daughter correlated recoil-decay tagged γ -ray spectrum for the ground-state decay of ^{172}Au . Three peaks are assigned to ^{172}Au and are listed in the lower part of Table II. The observation of different γ rays when tagging on the 6762-keV α decay of ^{172}Au provides further evidence that these decays emanate from a different state.

Although a full γ - γ coincidence study of ^{172}Au is prevented due to insufficient statistics, a tentative partial level scheme for ^{172}Au built on the isomeric state, has been constructed (Fig. 9). In Fig. 10 the spectra gated by the 363-, 460-, and 545-keV γ -ray transitions in this limited coincidence analysis

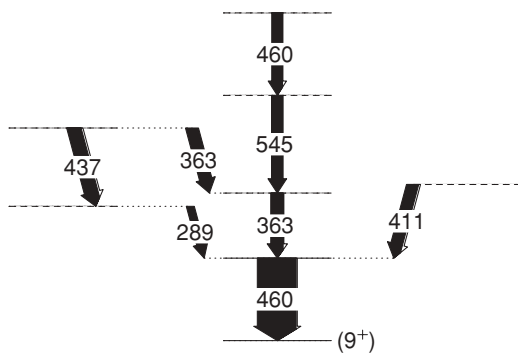


FIG. 9. A tentative level scheme for ^{172}Au built on the isomeric α -decaying state. The thickness of the arrows indicates the relative intensities of the transitions in the α -gated spectrum disregarding corrections for internal conversion.

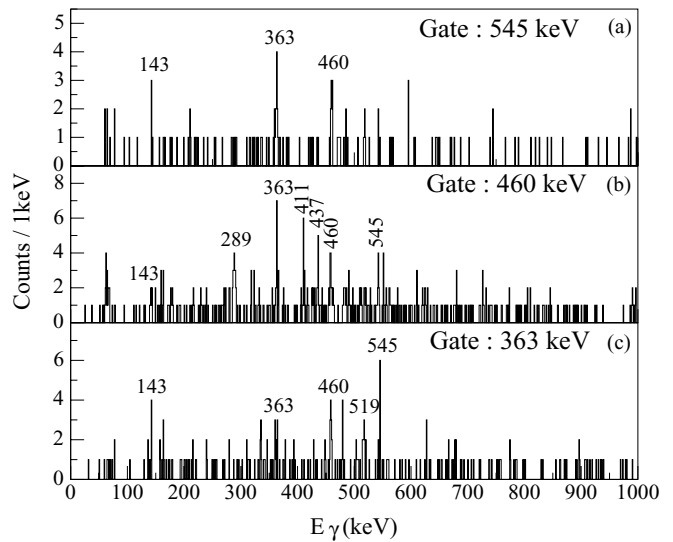


FIG. 10. Spectra gated by the (a) 545-keV, (b) 460-keV, and (c) 363-keV γ -ray transitions in $^{172}\text{Au}^m$.

are shown. The presence of doublets among the strongest transitions adds additional complexity in deducing a firm level structure for ^{172}Au . In the presented level scheme the ordering of the 289- and 437-keV transitions as well as the 545-keV and the upper 460-keV transitions were chosen based on their relative intensity when applying coincident gates on other transitions in their respective cascades. Since the effect of internal conversion on the intensities has not been taken into account, due to lack of firm knowledge on the multipolarity of these transitions, they were placed in the level scheme tentatively.

IV. DISCUSSION

The new results obtained from the decay studies in this work allow a systematic overview of the Q values in the region. Figure 11 displays the α -decay Q values for ^{172}Au , ^{168}Ir ,

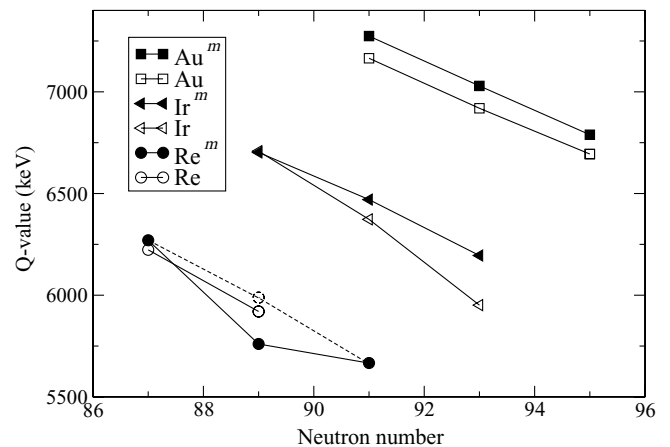


FIG. 11. The α -decay Q values for the low- and high-spin decaying states in ^{172}Au , ^{168}Ir , and ^{164}Re are plotted versus neutron number. Data are taken from Refs. [1,22,23]. See the text for details on the dashed line.

and ^{164}Re as well as their neighboring isotopes. It is seen that the smooth trend of decreasing Q values as a function of increasing neutron number is violated for the new datum for the decay of $^{164}\text{Re}^{(m)}$. However, there are two counts at 5846 keV in the spectrum shown in Fig. 2(g) that are indicated by the solid circle. If these were to represent the lowest lying state of $^{164}\text{Re}^{(m)}$ to the lowest lying state of $^{160}\text{Ta}^{(m)}$ then the smooth trend would be restored. This can be seen from the dashed line in Fig. 11 that connects the value for this tentative α -decay line, indicated by the dashed open circle, with those of neighboring isotopes. A reduced intensity for a certain α -decay branch may indicate a large spin change between the initial and final states or a significant change in configuration. If the tentatively proposed α decay at 5846 keV connects the lowest lying isomeric states in rhenium and tantalum, a change in structure is likely in the decay of $^{164}\text{Re}^{(m)}$ to $^{160}\text{Ta}^{(m)}$. The possibility of such a configuration change in $\text{Ta}^{(m)}$ relative to the other members of this α -decay chain requires further study.

The results presented in this work complete the decay chains originating from low-lying states in ^{172}Au down to corresponding states in ^{152}Tm . Recently, Litvinov *et al.* reported many atomic mass measurements including values for ^{152}Tm and ^{151}Er [24]. Unfortunately, there was some uncertainty with the measurement for ^{152}Tm caused by interference from another ion species having a similar mass-to-charge ratio. This is reflected in the somewhat larger than normal error of 54 keV for this nuclide. Furthermore, it is not clear whether the ^{152}Tm mass was deduced for the low-spin state, the high-spin state, or a mixture of the two, since they are probably close in energy as in ^{151}Tm and ^{153}Tm [15], and may not have been resolved in the mass measurement. Notwithstanding this uncertainty, it is possible to estimate the masses of some of the states in the decay chains and their proton-decay Q values, depending on which mass was measured. If the measured mass was for the low-spin state in ^{152}Tm , then combined with the Q values measured in the present work and those from Ref. [1], Q values for proton emission of 849, 534, and 131 keV can be deduced for the low-spin states in ^{172}Au , ^{168}Ir , and ^{164}Re , respectively. Although all three states would be proton unbound, their partial half-lives for proton emission would be too long to compete effectively with α decay. Alternatively, if it was the high-spin state in ^{152}Tm that was measured in Ref. [24], the corresponding proton-decay Q values for the high-spin states in these nuclei would be 1328, 902, and 407 keV, respectively. These estimates assume that the two counts discussed above represent the highest energy transition in ^{164}Re . These Q values suggest that any proton-decay branches from the high-spin states of these nuclei could have been just below the detection sensitivity of the present study, especially given the strong dependence of proton-decay half-lives on the decay energy and the size of the Q -value error bars. Clearly, it would be of interest to measure precisely the masses of both isomers in ^{152}Tm , or indeed any other member of these decay chains, to settle this question.

For neutron deficient nuclei in this mass region the proton orbitals $\pi h_{11/2}$, $\pi d_{3/2}$, and $\pi s_{1/2}$ and the neutron orbitals $\nu h_{9/2}$, $\nu f_{7/2}$, and $\nu i_{13/2}$ are close to the Fermi surface. For the odd- Z , even- N neighboring nuclei, generally two

α -decaying states are observed and assigned to originate from the $\pi h_{11/2}$ and $\pi(s_{1/2}, d_{3/2})$ configurations. For instance, the configuration of the α -decaying ground state in ^{169}Ir is proposed to be an equal mixture of the $\pi s_{1/2}$ and $\pi d_{3/2}$ orbitals, while the isomeric α -decaying state is assigned a $\pi h_{11/2}$ configuration [25]. In ^{170}Ir the configuration $\pi h_{11/2} \otimes \nu i_{13/2}$ is suggested to appear at an excitation energy of 500 keV relative to the isomeric α -decaying state [23]. Therefore, $\pi h_{11/2} \otimes \nu i_{13/2}$ and $\pi(s_{1/2}, d_{3/2}) \otimes \nu i_{13/2}$ or $\pi h_{11/2} \otimes \nu(f_{7/2}, h_{9/2})$ and $\pi(s_{1/2}, d_{3/2}) \otimes \nu(f_{7/2}, h_{9/2})$ are the most likely single-particle configurations for the α -decaying isomeric state and the ground state of ^{172}Au , respectively.

In the ^{174}Au and ^{176}Au isotopes, the tentatively assigned spins and parities are 9^+ and 3^- for the isomeric and ground states, respectively [26]. Considering the deformation parameters ($\beta_2 = 0.12$, $\gamma = -85^\circ$ for ^{174}Au and $\beta_2 = 0.13$, $\gamma = -85^\circ$ for ^{176}Au) obtained from total Routhian surface (TRS) calculations presented in the work by Goon [26], the assigned spins were given by the coupled Nilsson configurations $\pi h_{11/2}(\frac{1}{2}[505]) \otimes \nu f_{7/2}(\frac{7}{2}[503])$ for the high-spin isomeric state and $\pi d_{3/2}(\frac{1}{2}[411]) \otimes \nu f_{7/2}(\frac{7}{2}[503])$ for the ground state. The ^{172}Au nucleus might show an analogous structure. In ^{170}Au , the configurations $[\pi d_{3/2}\nu f_{7/2}]_{2-}$ and $[\pi h_{11/2}\nu f_{7/2}]_{9+}$ for the ground and the isomeric states have been suggested [5], which are the same as the preliminary assignments in ^{166}Ir [20].

To investigate the theoretical predictions for the structure of ^{172}Au , TRS [27] calculations for this nucleus were performed. The results of the TRS calculations for various parity and signature configurations present only small differences in the locations of the energy minima in the β_2 - γ plane. Therefore, the configuration assignments cannot be made with certainty. Figure 12 (left) illustrates the potential energy surface corresponding to the configuration $\pi(-, -1/2)$, $\nu(-, -1/2)$ involving an $h_{11/2}$ proton and an $f_{7/2}h_{9/2}$ neutron configuration that might be assigned to the high-spin isomeric state. The lowest minimum corresponds to a noncollective shape with $\beta_2 = 0.12$, $\gamma \approx -100^\circ$. The collective γ -soft minimum at $\beta_2 = 0.12$, $\gamma \approx 20^\circ$ is predicted to be slightly higher in excitation energy (only about 40 keV), which is well within the

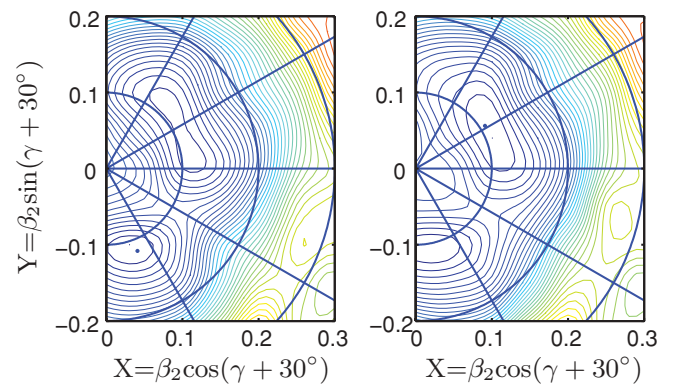


FIG. 12. (Color online) Total Routhian surfaces calculated at a rotational frequency of $\hbar\omega = 0.0$ MeV, for the configuration $\pi(-, -1/2)$, $\nu(-, -1/2)$ (left) and $\pi(+, +1/2)$, $\nu(-, -1/2)$ (right) for ^{172}Au are shown. Noncollective and collective energy minima are visible at weakly deformed shapes ($\beta_2 = 0.12$, $\gamma = -100^\circ$ and $\beta_2 = 0.11$, $\gamma = 0^\circ$) (see the text for more details).

expected uncertainty of the calculation. The TRS calculation for the configuration $\pi(+, +1/2)$, $\nu(-, -1/2)$ involving an $s_{1/2}d_{3/2}$ proton and a mixed $f_{7/2}h_{9/2}$ neutron configuration produces a minimum at $\beta_2 = 0.11$ and $\gamma \approx 0^\circ$, which might be assigned to the low-spin ground state [Fig. 12 (right)]. The results of the TRS calculations for the configurations involving the occupied $i_{13/2}$ neutron orbital instead of the $f_{7/2}$ orbital give minima that are predicted to be about 150–380 keV higher in energy at similar deformations. Therefore, considering the uncertainties in the calculations, the $i_{13/2}$ neutron is also a possible candidate for the configuration assignments for the isomeric and ground states in ^{172}Au . As mentioned above, the extraction of a firm level structure for ^{172}Au is prevented due to insufficient statistics and consequently a certain interpretation of the structure is difficult. However, the apparent absence of a low-lying rotational structure in ^{172}Au is in agreement with the results of the TRS calculations that predict a near-spherical shape for this nucleus. This is also in agreement with the systematics of light odd-odd Au isotopes (see below).

Comparing the odd-mass isotopes of neutron-deficient gold isotopes shows a change from low-lying rotational structures in ^{175}Au – ^{177}Au to low-lying irregular level structures in ^{171}Au – ^{173}Au [6,21]. This change is reflected in the energy difference between configurations corresponding to the $h_{11/2}$ and the $i_{13/2}$ proton orbitals as discussed by Bäck *et al.* [6]. A rapid increase in the energy of the excited level involving the $i_{13/2}$ proton is observed as the neutron number decreases [21]. Therefore, the rotational band with the $\pi i_{13/2}$ character is pushed up in energy and has not been observed in the lightest gold isotopes with odd mass number. Furthermore, no evidence for collective bands built on the $h_{11/2}$ proton configuration has been found in these isotopes [6,21].

For even- A gold isotopes irregular structures have been tentatively reported also in $^{174,176}\text{Au}$ [26]. The ^{182}Au nucleus is the lightest known odd-odd gold isotope that displays a collective rotational structure [7]. No data for the level structures of the odd-odd gold isotopes with mass numbers 178 and 180 are available. Therefore, from the systematics overview the absence of low-lying collective behavior in ^{172}Au is expected.

As the number of protons increases when moving toward the $Z = 82$ shell closure, the number of proton holes that can be involved in collective motion decreases. The fact that evidence for low-lying collective motion has not been observed in ^{172}Au (with three holes outside the closed $Z = 82$ shell) in comparison with its isotone $Z = 78$ ^{171}Pt (with four holes outside the closed shell) that exhibits collective rotational structure [28] points to a pronounced contribution of each valence proton hole for generating collective motion in this region.

Furthermore, in ^{170}Ir , the $Z = 77$ isotone of ^{172}Au , a strongly coupled rotational band has been observed at an excitation energy of 500 keV, with a tentatively assigned configuration of $\pi h_{11/2} \otimes \nu i_{13/2}$. The level structures of light odd-

A iridium isotopes have been firmly established and strongly coupled rotational bands with $\pi h_{11/2}$ character have been reported in ^{169}Ir and ^{171}Ir [25,29]. The fact that no evidence for a rotational structure involving the $\pi h_{11/2}$ configuration has been observed in the gold isotopes [6,21], in contrast to the corresponding iridium isotones, also demonstrates the shape-polarizing effect of the two additional proton holes. This feature might possibly also reflect the effect of an increased quadrupole component of the proton-neutron interactions (which increase with $N_n \cdot N_p$, the product of the number of valence protons and neutrons relative to the nearest closed shell [30,31]), resulting in enhanced low-lying collectivity. In our TRS calculations a corresponding trend is seen, with a decrease in the deformation parameter β_2 from 0.15 in ^{170}Ir [23] to 0.13 in ^{172}Au for the $\pi h_{11/2} \otimes \nu i_{13/2}$ configuration.

V. SUMMARY

The α decays of the low-spin ground state of ^{172}Au and the high-spin isomer in ^{164}Re have been observed for the first time, allowing continuous decay chains from ^{172}Au to ^{152}Tm to be established. The observation of α -decay fine structure has made it possible to identify low-lying excited states in ^{168}Ir and ^{164}Re . Gamma-ray transitions depopulating excited states built on the α -decaying isomeric and ground states in ^{172}Au have been identified using the recoil-decay tagging method. A tentative level scheme built on the isomeric α -decaying state in ^{172}Au has been deduced. Several possible configuration assignments for the α -decaying states in ^{172}Au have been discussed in terms of systematics of the region and the results of TRS calculations.

ACKNOWLEDGMENTS

The authors thank the staff at the Accelerator Laboratory at the University of Jyväskylä for their excellent technical support. This work was supported through EURONS (European Commission Contract No. RII3-CT-2004-506065) and by Academy of Finland under the Finnish Centre of Excellence Programme 2006-2011 (Nuclear and Accelerator-Based Physics Contract No. 213503). Further support for this work has been provided by the Swedish Research Council, the Göran Gustafsson Foundation, the United Kingdom Science and Technology Facilities Council, the United Kingdom Engineering and Physical Sciences Research Council, the European Union Fifth Framework Programme “Improving Human Potential—Access to Research Infrastructure” (Contract No. HPRI-CT-1999-00044), and by the JSPS Core-to-Core Program, International Research Network for Exotic Femto Systems (EFES). We also thank the UK Science and Technology Facilities Council/France (STFC/IN2P3) detector Loan Pool and EUROBALL owners committee (GAMMAPOOL network) for the EUROGAM detectors of JUROGAM.

[1] R. D. Page *et al.*, Phys. Rev. C **53**, 660 (1996).

[2] G. L. Poli *et al.*, Phys. Rev. C **59**, R2979 (1999).

[3] E. S. Paul *et al.*, Phys. Rev. C **51**, 78 (1995).

[4] R. S. Simon *et al.*, Z. Phys. A **325**, 197 (1986).

[5] H. Kettunen *et al.*, Phys. Rev. C **69**, 054323 (2004).

[6] T. Bäck *et al.*, Eur. Phys. J. A **16**, 489 (2003).

- [7] Y. H. Zhang *et al.*, *Eur. Phys. J. A* **14**, 271 (2002).
- [8] P. J. Sellin *et al.*, *Z. Phys. A* **346**, 323 (1993).
- [9] C. W. Beausang *et al.*, *Nucl. Instrum. Methods A* **313**, 37 (1992).
- [10] M. Leino *et al.*, *Nucl. Instrum. Methods B* **99**, 653 (1995).
- [11] M. Leino, *Nucl. Instrum. Methods B* **126**, 320 (1997).
- [12] R. D. Page *et al.*, *Nucl. Instrum. Methods B* **204**, 634 (2003).
- [13] I. H. Lazarus *et al.*, *IEEE Trans. Nucl. Sci.* **48**, 567 (2001).
- [14] P. Rahkila, *Nucl. Instrum. Methods A* **595**, 637 (2008).
- [15] K. S. Toth and W. Nazarewicz, *Phys. Rev. C* **48**, R978 (1993).
- [16] C. Cabot *et al.*, *Z. Phys. A* **287**, 71 (1978).
- [17] S. Hofmann *et al.*, *Z. Phys. A* **299**, 281 (1981).
- [18] S. Hofmann *et al.*, *Z. Phys. A* **291**, 53 (1979).
- [19] P. J. Woods, C. N. Davids *et al.*, *Annu. Rev. Nucl. Part. Sci.* **47**, 541 (1997).
- [20] C. N. Davids *et al.*, *Phys. Rev. C* **55**, 2255 (1997).
- [21] F. Kondev *et al.*, *Phys. Lett.* **B512**, 268 (2001).
- [22] R. G. Helmer, *Nucl. Data Sheets* **101**, 325 (2004).
- [23] B. Hadinia *et al.*, *Phys. Rev. C* **76**, 044312 (2007).
- [24] Yu. A. Litvinov, *Nucl. Phys.* **A756**, 3 (2005).
- [25] M. Sandzelius *et al.*, *Phys. Rev. C* **75**, 054321 (2007).
- [26] T. M. Goon, Ph.D. thesis, The University of Tennessee, 2004.
- [27] W. Satula and R. Wyss, *Phys. Scr.* **T56**, 159 (1995).
- [28] D. Seweryniak *et al.*, *Phys. Rev. C* **58**, 2710 (1998).
- [29] D. Seweryniak *et al.*, *Nucl. Phys.* **A657**, 113 (1999).
- [30] R. F. Casten, *Nucl. Phys.* **A443**, 1 (1985).
- [31] R. F. Casten, *Inst. Phys. Conf. Ser. No. 88* [*J. Phys. G: Nucl. Phys.* 14 Suppl.]